Available online at www.sciencedirect.com
ScienceDirect
Journal of the European Ceramic Society 31 (2011) 281–290
www.elsevier.com/locate/jeurceramsoc

Texture coefficients for the simulation of cordierite thermal expansion: A comparison of different approaches

Alexander M. Efremov [a], Giovanni Bruno [b,*], Bryan R. Wheaton [b]

[a] *Corning OOO, Modeling and Simulation, CSC-St. Petersburg, Russia*
[b] *Corning Inc., CS&S, SP, Corning, NY, USA*

Received 15 June 2010; received in revised form 12 August 2010; accepted 2 October 2010
Available online 1 November 2010

Abstract

The dependence of the coefficient of thermal expansion (CTE) from the texture description in porous ceramics is presented, in the example of cordierite. The texture description usually adopted for industrial ceramics, the *I*-ratio, is compared with the more rigorous approach of neutron diffraction (ND) pole figures. It is shown that the use of the *I*-ratio represents a coarse approximation of the complete materials texture and it yields different values of the texture coefficients used to model the CTE from lattice expansion data (according to the integrity function). For extruded and fired samples, it is shown that if for the transverse direction all approximations are equivalent, for the axial CTE the usual *I*-ratio values bring contradictory simulation results. On the contrary, the use of ND pole figures and of the Popa–Bruno method allows predicting sensible CTE values, consistent with other physical properties, such as Young's modulus.

Keywords: Neutron and X-ray methods; Thermal expansion; Texture; Cordierite; Integrity factor

1. Introduction

Numerical simulations of thermo-mechanical properties have nowadays become a recognized path to understanding, predicting and improving of physical properties of ceramics. Particular targets for those calculations are materials for membranes and catalyst substrates applications, since they consist of highly anisotropic microcrystals. The simulation of bulk coefficient of thermal expansion (CTE) requires the input of microcrystal orientations in the ceramic body, besides the composition, and of the (generally anisotropic) intrinsic properties of the crystal phases. According to the constitutive model of polycrystalline material, the bulk CTE equals the weighted sum of the crystal axial CTE's where the weights include texture coefficients. The latter depend on the average orientation of crystals along the direction of thermal expansion (see for example [1–3]).

The current method for quick texture characterization of industrial ceramics uses X-ray diffraction (XRD).[4] In the case of cordierite the texture is evaluated in the most simple and practical way by a single value named *I*-ratio. The value equals the intensity of X-ray diffraction (XRD) reflection 1 1 0 normalized by the intensity sum of 1 1 0 and 0 0 2 reflections of the hexagonal form (indialite). In other words, this quantity aims at quantifying the amount of basal oriented *c*-grains with respect to the basal + axial orientations, i.e.

$$I_{ratio} = \frac{I_{110}}{I_{002} + I_{110}} \tag{1}$$

We notice two facts:

1. The intensity sum of 3 1 0 and 0 2 0 reflections, instead of the 1 1 0, should be taken for the most common orthorhombic cordierite; however, we could also define the *I*-ratio as

$$I^{L}_{ratio} = \frac{I_{310}}{I_{002} + I_{310}} \tag{1'}$$

since the intensity of 3 1 0 peak is not affected by the 0 2 0 peak.
2. Lachman[4] used the peak heights for definitions (1) and (1′), while Bubeck[5] used the integrated intensity (peak areas A_{hkl})

* Corresponding author. Tel.: +1 607 9741421; fax: +1 607 9742383.
E-mail address: brunog@corning.com (G. Bruno).

0955-2219/$ – see front matter © 2010 Elsevier Ltd. All rights reserved.
doi:10.1016/j.jeurceramsoc.2010.10.005

of 3 1 0 plus 0 2 0 peaks:

$$I^{B}_{ratio} = \frac{A_{310} + A_{020}}{A_{002} + A_{020} + A_{310}} \quad (1'')$$

(we attach labels *L* for Lachman and *B* for Bubeck to the two definitions).

However, the peak width is a smoothly varying function of the Bragg angle 2α (note that we use α to avoid confusion with the Euler polar angle, θ). Consequently, since the peaks 3 1 0, 0 2 0 and 0 0 2 are near each other, we can assume their width to be the same and write

$$I^{B}_{ratio} \sim \frac{I_{310} + I_{020}}{I_{002} + I_{020} + I_{310}} \quad (1''')$$

whereby the peak heights I_{hkl} are used.

Both approaches are equivalent, but the latter practice is more rigorous, since the peak area represents the whole contribution of the grains oriented in the direction under investigation.

According to the crystallographic databases (PDF file 89–1488, see [6]), the intensities of the three peaks in a variable slit geometry (which we use for the XRD measurements) are:

$$I_{310} = 28; \quad I_{020} = 14; \quad I_{002} = 14;$$

taking the definition (1′) would give for a randomly oriented powder reference $I_{\text{powder}} = 2/3$, while taking the sum of the 3 1 0 and 0 2 0 peaks (or the integrated intensities), definitions (1″) or (1‴), we would have $I_{\text{powder}} = 3/4$.

The practical convenience of this definition lies in that the two peaks are located around the same Bragg angle $2\alpha \sim 19^{\circ}$ in an X-ray diffraction pattern acquired for Cordierite with conventional Cu anode. The *I*-ratio value provides information about the amount of *a*- and *b*-axis contribution to the CTE in the specific sample direction of XRD inspection.

As stated in [4], the exact physical meaning can be addressed to the following cases: an $I_{\text{ratio}} = 0$ ($I_{110} = 0$) shows that all crystals are oriented with their *c*-axes perpendicular to sample surface and $I_{\text{ratio}} = 1$ ($I_{002} = 0$) denotes that there are no crystals with *c*-axis perpendicular to the sample surface.

When obtaining intermediate values, the *I*-ratio has been however erroneously used as an absolute texture metric. For example, Bubeck [5] used the *I*-ratio measured at various locations of honeycomb structures as weights (texture coefficients) for the calculation of the axial and radial CTEs. Estimated values were found at 200% the measured values. Such a mismatch could be related to the effect of thermal microcracking due to anisotropy of the crystallographic CTE [1], but certainly depends on the failure of the *I*-ratio to describe the fraction of oriented crystallites.

Indeed, we will see that several factors render the *I*-ratio only a qualitative description of the preferred orientation: for example, the scanty X-ray penetration depth and the variation of the crystal orientation as a function of depth in the walls could play a significant role in the assessment of the sample texture by the *I*-ratio method.

A rigorous mathematical method for averaging local physical properties using the crystallographic texture of anisotropic polycrystalline materials has been proposed by Popa [7] for the calculation of average strain (stress) and stiffness. In that work, the material texture is given by the fractional density of crystal orientations or orientation distribution function (ODF) versus the Euler angles, which relate the crystal coordinate system to that of the laboratory.

Bruno and Vogel [3] derived analytically the texture coefficients for fiber texture of transversely isotropic cordierite crystals ($a = b \neq c$). The fiber texture (axially symmetric distribution of the *c*-axis around the extrusion direction) was derived from pole figures obtained by neutron diffraction experiments on honeycomb and compact cordierite specimens.

The purpose of the work is to discuss the limitations of the *I*-ratio approach, compare the results of texture coefficients derivation from *I*-ratio and pole figure data, and observe their impact on the calculation of the radial and axial CTE in porous honeycomb ceramic material. We will see that the correct determination of the texture coefficients is capital for any model to approach the measured CTE values and therefore be *predictive*. As a test, the Turner's model [2], as modified by Efremov [1], will be used and compared to previous results.

2. Experimental details and theoretical approach

2.1. Materials and methods

Some honeycomb porous extruded cordierite was produced at Corning Inc. by sintering a mixture of talc, alumina, kaolin and silica at temperatures in excess of 1400 °C. This batch was characterized by Neutron and X-ray diffraction. The specimen was cut into cellular bars of dimensions about 12 mm × 12 mm × 30 mm for the ND and the XRD tests and into bars of about 5 mm × 5 mm × 50 mm for conventional dilatometry. Neutron diffraction experiments were run at the LANSCE, LANL, NM, USA on the instrument HIPPO (see [3,8]). X-ray diffraction experiments were run at the X-ray laboratory of Corning Inc., Sullivan Park, Corning, NY, USA, on a Panalytical X'Pert diffractometer equipped with Cu Kα anode. Complementarily, standard dilatometry experiments were run on a Neztsch DL402 single pushrod dilatometer at Corning SAS, CETC, Avon, France.

2.2. Theoretical considerations

2.2.1. Limitations of the I-ratio approach

In spite of its convenience for industry, the *I*-ratio approach has certain limitations.

(1)- As seen in the introduction, the *I*-ratio corresponding to a random orientation distribution would change according to the definition and the crystallographic database we use. Moreover, experimental values reported in the literature for isotropic powder samples are different (0.664 is obtained in [4], 0.75 is reported in [5]) if we use peak height or area. The different diffraction angle for *a* and *b*-axes (1 1 0 line, $2\alpha \sim 18.15^{\circ}$) and *c*-axis (0 0 2 line, $2\alpha \sim 19.1^{\circ}$) may also play a role, if absorption and

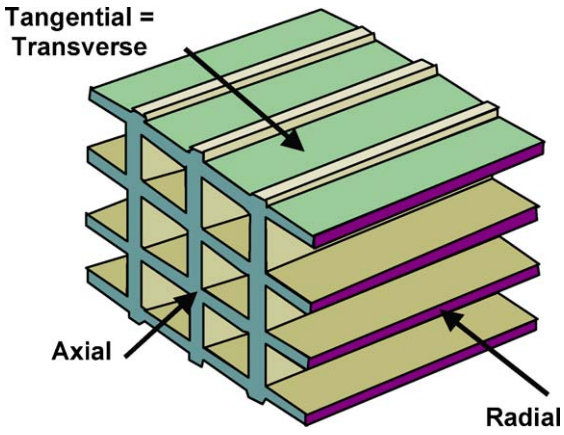

Fig. 1. The nomenclature used for the *I*-ratio determination by X-ray diffraction.

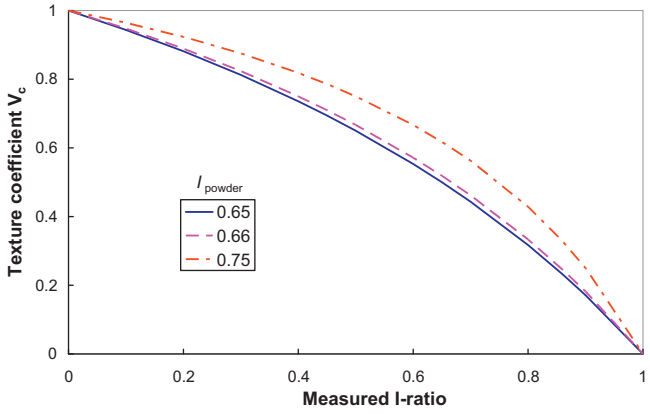

Fig. 2. V_c as a function of the measured *I*-ratio for different I-powder values of 2/3 (dashed line), 0.65 (present work, solid line) and 0.75 (value found in [5], dash-dotted line).

polarization factors are not properly taken into account [9,10].

In order to avoid the limitation, it will be shown below that we suggest a formula for calibration of measured *I*-ratio, assuming the measured powder is purely random oriented. Calibration can be done for any value of the theoretical powder *I*-ratio value.

(2)- X-ray Cu Kα penetration depth in porous cordierite is limited to a thin layer of about 10 μm. This would be sufficient for texture inspection only in the case, where the layer perpendicular to the investigated direction could adequately represent volume orientations. However, this depth is not enough to characterize most of the cellular (honeycomb) sample directions (see definition in Fig. 1), due to the significant difference of crystal alignment at the surface and inside the core of a wall [4,5]. On the contrary, we would need a meaningful volume average of the microscopic properties, if we want to extract macroscopic properties (such as CTE or Young's modulus) via models. This is why the use of neutrons (or high energy synchrotron radiation) as a probe for texture analysis yields a significant advantage: since the measured volume can be of the order of several cm^3, the statistical average of microscopic properties (such as strain or crystal texture) can be used to extract macroscopic properties (such as stiffness or CTE).

(3)- A thorough description of the crystallographic texture or a polycrystal (or the so-called orientation distribution function, ODF) cannot be done using just two/three reflections (3 1 0, 0 2 0 and 0 0 2) [11]. Consequently, the *I*-ratio is not representative of the complete ODF, as most of the crystal population does not contribute to the *I*-ratio value. This is particularly true if XRD is carried out, because the statistical ensemble of grains involved in the experiment could be very small.

Whereas the first limitation related to interpretation of measured *I*-ratio can be resolved as shown in the next section, the other two cannot be overcome, due to simple physical reasons.

Instead, we will see that pole figures, as obtained by neutron diffraction, yield a meaningful statistical average, thanks to the high penetration depth of neutrons. Moreover, measurements on several Bragg peaks yield more complete information about the crystal orientation *distributions* around the sample axes of interest, and therefore allow calculating correct averages of physical quantities.

2.2.2. Texture coefficients derivation from I-ratio

The *I*-ratio value obtained from XRD experiments, currently used in industrial applications for the description of cordierite texture, is given by Eq. (1) or (1′).

On the basis of the theoretical ratio, we developed a relation between the measured I_{ratio}, that of a powder (I_{powder}) and the texture weight to insert in current models, which we call the texture coefficient V_c in the following. The relation reads

$$V_c = \frac{1 - I_{ratio}}{1 - \left(2I_{powder} - 1/I_{powder}\right) \cdot I_{ratio}} \tag{2}$$

Fig. 2 shows the variation of V_c as a function of the *I*-ratio for a solid sample when I_{powder} equals 2/3 (dashed line), 0.65 (solid line), and 0.75 (dash-dot line). The first value corresponds to the use of definition (1′), the latter value has been reported by Bubeck[5] and corresponds to the use of the 3 1 0, 0 2 0 and 0 0 2 peaks (areas or heights).

The meaning of Eq. (2) is the following: for a correct comparison of the *I*-ratio values obtained in different experiments one has to calibrate these values by referring them to the experimental *I*-ratio of a powder, supposed to have isotropic orientation. As mentioned above, we can calibrate the measured *I*-ratio to theoretical values of 2/3 (according to [4]) and 3/4 (according to [5]). We therefore get in the two cases:

$$\begin{aligned} I^{cal}(I^{meas}, I_{powder}) &:= \frac{2 \cdot ((1/I_{powder}) - 1) \cdot I^{meas}}{1 - (3 - (2/I_{powder})) \cdot I^{meas}} \quad I^{th}_{ratio} = 2/3 \\ I^{cal}(I^{meas}, I_{powder}) &:= \frac{3 \cdot ((1/I_{powder}) - 1) \cdot I^{meas}}{1 - (4 - (3/I_{powder})) \cdot I^{meas}} \quad I^{th}_{ratio} = 3/4 \end{aligned} \tag{3}$$

The texture coefficient can then be calculated by means of Eq. (2) in both cases.

The details of the derivation of Eqs. (2) and (3) are given in Appendix A. Incidentally, we note that Bubeck [5] implicitly calibrated his *I*-ratio values, by referring the CTE to different samples and extrapolating to axial and radial mixtures.

2.2.3. Texture coefficients derivation from pole figures

2.2.3.1. The texture coefficients of a grain. The (thermal) strain tensor of an orthotropic grain in its own coordinate system (a, b, c) is given by

$$\varepsilon_g(\varepsilon_a,\varepsilon_b,\varepsilon_c) := \begin{pmatrix}\varepsilon_a & 0 & 0\\ 0 & 0 & 0\\ 0 & 0 & 0\end{pmatrix} + \begin{pmatrix}0 & 0 & 0\\ 0 & \varepsilon_b & 0\\ 0 & 0 & 0\end{pmatrix} + \begin{pmatrix}0 & 0 & 0\\ 0 & 0 & 0\\ 0 & 0 & \varepsilon_c\end{pmatrix} = \begin{pmatrix}\varepsilon_a & 0 & 0\\ 0 & \varepsilon_b & 0\\ 0 & 0 & \varepsilon_c\end{pmatrix} \quad (4)$$

The expression of this tensor in the laboratory system can be expanded as a sum of contributions transformed according to the tensorial law of transformation using the Euler angles ψ, θ, ϕ (see Appendix B), i.e.

$$\begin{aligned}&\varepsilon(\psi,\theta,\phi,\varepsilon_a,\varepsilon_b,\varepsilon_c)\\ &:= T(\psi,\theta,\phi)\cdot\varepsilon_g(\varepsilon_a,\varepsilon_b,\varepsilon_c)\cdot T^T(\psi,\theta,\phi)\\ &= v_a\varepsilon_a + v_b\varepsilon_b + v_c\varepsilon_c\end{aligned} \quad (5)$$

The grain contribution to the texture coefficients are given by

$$\begin{aligned}v_a(\varepsilon_a,\varepsilon_b,\varepsilon_c) &= \varepsilon(\psi,\theta,\phi,1,0,0)\\ v_b(\varepsilon_a,\varepsilon_b,\varepsilon_c) &= \varepsilon(\psi,\theta,\phi,0,1,0)\\ v_b(\varepsilon_a,\varepsilon_b,\varepsilon_c) &= \varepsilon(\psi,\theta,\phi,0,0,1)\end{aligned} \quad (6)$$

One can verify that the sum of texture coefficients of a single grain equals 1 (see details in Appendix B):

$$v_a(\varepsilon_a,\varepsilon_b,\varepsilon_c) + v_b(\varepsilon_a,\varepsilon_b,\varepsilon_c) + v_b(\varepsilon_a,\varepsilon_b,\varepsilon_c) = \begin{pmatrix}1 & 0 & 0\\ 0 & 1 & 0\\ 0 & 0 & 1\end{pmatrix} \quad (7)$$

2.2.3.2. The average texture coefficient in polycrystalline materials. In general, the average of a physical quantity weighted by the crystal orientation has been treated by Balzar and Popa [7], using the formalism of Bunge [11]. In our case, for texture representation let us introduce the crystal orientation distribution function $f(\psi,\theta,\phi)$. This function is normalized in the Euler space by

$$\frac{1}{8\pi^2}\iiint f(\psi,\theta,\phi)\cdot d\psi d\theta d\phi = 1 \quad (8)$$

The average of a quantity $\varepsilon_{\mathrm{Lab}}$ over the crystallite orientation distribution function is given by $\varepsilon_{\mathrm{macro}}$, such that:

$$\begin{aligned}\varepsilon_{macro} &= \frac{1}{8\pi^2}\iiint f(\psi,\theta,\phi)\cdot\varepsilon_{Lab}(\psi,\theta,\phi,\varepsilon_a,\varepsilon_b,\varepsilon_c)\cdot d\psi\cdot d\theta\cdot\\ d\phi &= \frac{1}{8\pi^2}\iiint f(\psi,\theta,\phi)\cdot[v_a(\psi,\theta,\phi)\cdot\varepsilon_a + v_b(\psi,\theta,\phi)\cdot\varepsilon_b\\ &+ v_c(\psi,\theta,\phi)\cdot\varepsilon_c]\cdot d\psi\cdot d\theta\cdot d\phi\end{aligned} \quad (9)$$

Which means:

$$\varepsilon_{macro} = V_a\cdot\varepsilon_a + V_b\cdot\varepsilon_b + Vc\cdot\varepsilon_c \quad (10)$$

where V_i are defined as

$$V_i = \frac{1}{8\pi^2}\iiint f(\psi,\theta,\phi)\cdot v_i\cdot d\psi\cdot d\theta\cdot d\phi; \quad i = a,b,c \quad (11)$$

With these equations one can demonstrate that $V_a + V_b + V_c = 1$ in any sample direction (ax, rad, hoop) and for every $f(\psi,\theta,\phi)$. The proof is given in Appendix B.

Finally, we must note that the texture coefficients of each single crystal axis (a, b or c) calculated from pole figures are already normalized, by virtue of their definition, while those extracted from the I-ratio treatment must be normalized to 1 according to

$$V_c^n(i) = \frac{V_c(i)}{\sum_j V_c^n(j)} \quad (12)$$

whereby V_c are the calculated texture coefficients and i,j run over the axial, radial and tangential directions. In the following, only normalized texture coefficients will be used and the suffix n omitted for clarity.

3. Results

3.1. Results of XRD experiments

The measured (XRD) and calibrated I-ratio values for a cellular sample are presented in Table 1. The correspondent I-ratios measured on a powder are also indicated. A pseudo-Voigt function was used to fit the peaks, but the peak intensities (and not the areas) were used, as mentioned above.

3.2. Results of neutron diffraction experiment

The complete pole figures for the honeycomb sample, as measured by neutron diffraction at the Lujan Neutron Scattering Center, Los Alamos, NM, USA are shown in Fig. 3, see also [3].

The cordierite pole figure for the c-axis, obtained by neutron diffraction experiments [3], was then approximated by an axially symmetric (dependent on θ only) Gaussian texture function $I(\theta)$, θ polar angle, given by

$$I(\theta) = \frac{\pi}{2}\cdot\exp\left[-\frac{1}{2}\cdot\left(\frac{\theta}{\Delta\theta}\right)^2\right] + I_0 \quad (13)$$

Table 1
Results of XRD experimental and calibrated I-ratio.

I_{ratio}	Tangential	Radial	Axial	I_{powder}
Measured, def. (1′)	0.86	0.57	0.45	0.65
Calibrated, def. (1′)	0.87	0.59	0.47	0.666
Measured, def. (1″)	0.90	0.66	0.53	0.74
Calibrated, def. (1″)	0.90	0.67	0.54	0.75

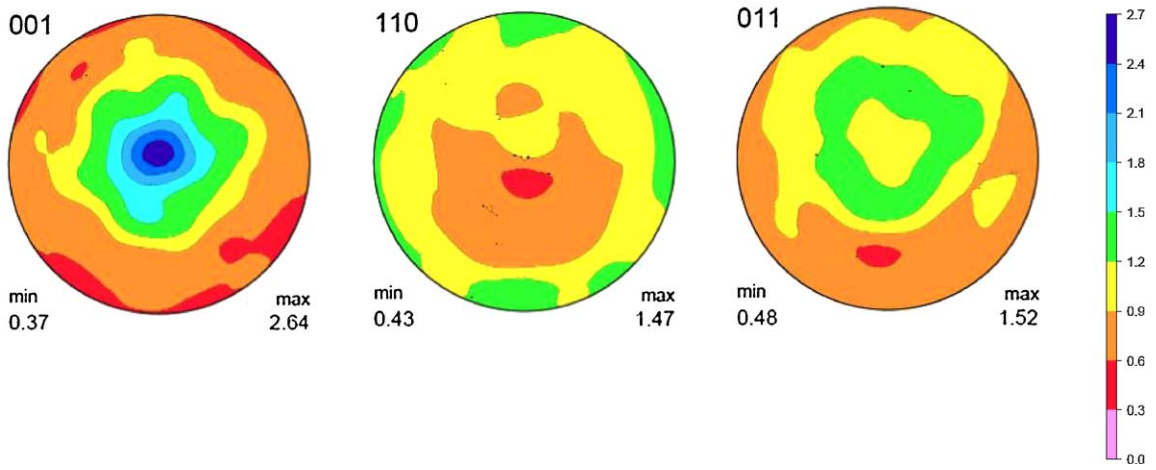

Fig. 3. Pole figures for the cellular cordierite material, as measured by neutron diffraction (see also [3]). The texture index is 1.2 (i.e. the global texture is weak). The extrusion axis is in the center of the pole figures.

With $\Delta\theta = 28.1^\circ$ and $I_0 = .69$ is the random (isotropic) background.

The function $I(\theta,\Delta\theta)$ was normalized so that $I_p = C\,I$ and

$$\frac{1}{8\pi^2}\iiint C\cdot I\,(\psi,\theta,\phi)\cdot d\psi\cdot d\theta\cdot d\phi = \frac{1}{8\pi^2}\iiint I_p\,(\psi,\theta,\phi)\cdot d\psi\cdot d\theta\cdot d\phi = 1 \tag{14}$$

This yielded to $C = 1.097$. The function I_p is plotted in Fig. 4.

Now, in order to calculate the contribution of the CTE in the *axial* (z) direction, we need to evaluate the texture coefficients given by the integrals:

$$\begin{aligned} V_a &= \frac{1}{8\pi^2}\iiint I_p\,(\theta,\Delta\theta)\cdot v_a(\psi,\theta,\phi)_{3,3}\cdot\sin\theta\cdot d\psi\cdot d\theta\cdot d\phi = 0.293\\ V_b &= \frac{1}{8\pi^2}\iiint I_p\,(\theta,\Delta\theta)\cdot v_b(\psi,\theta,\phi)_{3,3}\cdot\sin\theta\cdot d\psi\cdot d\theta\cdot d\phi = 0.293\\ V_c &= \frac{1}{8\pi^2}\iiint I_p\,(\theta,\Delta\theta)\cdot v_c(\psi,\theta,\phi)_{3,3}\cdot\sin\theta\cdot d\psi\cdot d\theta\cdot d\phi = 0.415 \end{aligned} \tag{15}$$

Which, incidentally, satisfy the condition $V_a + V_b + V_c = 1$.

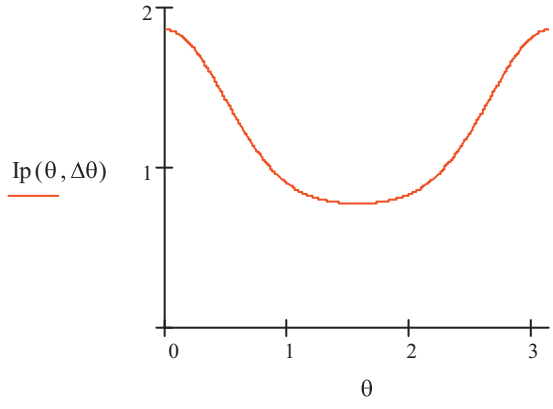

Fig. 4. The normalized texture function $I_p(\theta)$, as determined by neutron diffraction (θ is in radians).

Analogously, the contribution in the *tangential* (x) direction is such that

$$\begin{aligned} V_a &= \frac{1}{8\pi^2}\iiint I_p\,(\theta,\Delta\theta)\cdot v_a(\psi,\theta,\phi)_{1,1}\cdot\sin\theta\cdot d\psi\cdot d\theta\cdot d\phi = 0.354\\ V_b &= \frac{1}{8\pi^2}\iiint I_p\,(\theta,\Delta\theta)\cdot v_b(\psi,\theta,\phi)_{1,1}\cdot\sin\theta\cdot d\psi\cdot d\theta\cdot d\phi = 0.354\\ V_c &= \frac{1}{8\pi^2}\iiint I_p\,(\theta,\Delta\theta)\cdot v_c(\psi,\theta,\phi)_{1,1}\cdot\sin\theta\cdot d\psi\cdot d\theta\cdot d\phi = 0.293 \end{aligned} \tag{16}$$

Which again satisfy the condition $V_a + V_b + V_c = 1$.

The contribution to the *radial* (y) direction is such that

$$\begin{aligned} V_a &= \frac{1}{8\pi^2}\iiint I_p\,(\theta,\Delta\theta)\cdot v_a(\psi,\theta,\phi)_{2,2}\cdot\sin\theta\cdot d\psi\cdot d\theta\cdot d\phi = 0.354\\ V_b &= \frac{1}{8\pi^2}\iiint I_p\,(\theta,\Delta\theta)\cdot v_b(\psi,\theta,\phi)_{2,2}\cdot\sin\theta\cdot d\psi\cdot d\theta\cdot d\phi = 0.354\\ V_c &= \frac{1}{8\pi^2}\iiint I_p\,(\theta,\Delta\theta)\cdot v_c(\psi,\theta,\phi)_{2,2}\cdot\sin\theta\cdot d\psi\cdot d\theta\cdot d\phi = 0.293 \end{aligned} \tag{17}$$

With $V_a + V_b + V_c = 1$.

The texture coefficients shown in Eqs. (14)–(16) obtained from the texture function (13) are summarized in Table 2.

One can see that Tangential and Radial coefficients coincide and $V_a = V_b$ in all lab (XYZ) directions because of the texture function symmetry that here depends on θ only·

Table 2
Texture coefficients V_i calculated from the c-axis texture function deduced from neutron diffraction measurements.

	V_a	V_b	V_c
Axial (Z)	0.293	0.293	0.415
Tangential (X)	0.354	0.354	0.293
Radial (Y)	0.354	0.354	0.293

4. Discussion

4.1. I_{ratio} from ND pole figures

In the case of ND measurements, the radial and tangential directions cannot be distinguished, because of the axial symmetry: neutrons take the signal from all walls oriented in the diffraction condition and therefore the radial and tangential orientations are averaged together. In particular, this means that limitation (2) mentioned above is overcome for the *I*-ratio derived from pole figure.

Bearing in mind that the texture coefficient sum equals 1, we can estimate the axial and radial *I*-ratios from the one-dimensional distribution function I_p derived from the 0 0 1 pole figure. To make an analogous calculation to the *I*-ratio concept, we have to assume that only the reflections 0 0 1, 1 0 0 and 0 1 0 contribute to the diffraction signal. In this case, the sum of the intensities is given by

$$I_{sum} = I_p(0, \Delta\theta) + 2 \cdot I_p\left(\frac{\pi}{2}, \Delta\theta\right) \tag{18}$$

we then obtain the calibrated Axial and Radial *I*-ratios as follows,

$$\begin{aligned} I_{ratio}(\text{Axial}) &= \frac{I_{sum} - I_p(0, \Delta\theta)}{I_{sum}} = 0.452 \\ I_{ratio}(\text{Radial}) &= \frac{I_{sum} - I_p((\pi/2), \Delta\theta)}{I_{sum}} = 0.774 \end{aligned} \tag{19}$$

One can see that the *I*-ratio values defined this way satisfy the condition:

$$1 - I_{ratio}(\text{Axial}) + 2 \cdot (1 - I_{ratio}(\text{Radial})) = 1 \tag{20}$$

In the case of X-rays, the cellular geometry yields different signals (and different averages) in the radial and tangential directions, as exemplified in Table 1.

4.2. Comparison between XRD and ND I-ratio

In accordance to what we discussed above, the Tangential *I*-ratio turns out to be higher at the surface (XRD) than on the average (ND) value, Table 3. Moreover, as outlined before, the ND values contain the average of radial and tangential signals.

However, this difference can be explained by the different way we described the *I*-ratio for neutrons and X-rays experiments that only coincide if the 0 1 0 and 0 0 1 orientations are the same:

$$\begin{aligned} I_{ratio} &= \frac{I_{110}}{I_{002} + I_{100}} \quad \text{X-rays} \\ I_{ratio} &= \frac{2I_{100}}{I_{001} + 2I_{100}} \quad \text{Neutrons} \end{aligned} \tag{21}$$

Table 3
Calibrated *I*-ratio as obtained from XRD and ND pole figure.

Cordierite I_{ratio}	Axial	Radial	Tang
XRD	0.47	0.59	0.87
ND (001 pole figure)	0.45	0.77	0.77

Table 4
Texture coefficients V_c as obtained from XRD and ND *I*-ratio and pole figure.

Cordierite V_c	Axial	Radial	Tang
XRD (*I*-ratio)	0.47	0.38	0.16
ND (*I*-ratio)	0.49	0.26	0.26
ND (pole figure)	0.41	0.29	0.29

4.3. Comparison between texture coefficients based on XRD and ND data

The Axial texture coefficient V_c obtained from the whole information conveyed by the pole figure, i.e. calculated using the Popa method (as simplified by Bruno [3], Eq. (16)), is $V_c = 0.41$ versus 0.47 obtained from XRD *I*-ratio and 0.49 from ND *I*-ratio (Tables 3 and 4). Indeed, the latter approximations are both missing most crystallites oriented in directions other than that inspected, in accordance with the limitation (3). Table 4 shows the impact of the approximations done using the different data sets: note that ND is free of limitation (2) and (3) above, while XRD is not.

4.4. Calculation of CTE with texture coefficients

At this point, we can calculate (Fig. 5) the average axial and radial CTE (and/or the dilation) of an ideally intact material, using the texture coefficients of Table 4 and the lattice expansion data available in the literature (see [12]). The model set forth in [1] has been used.

One important point must be raised before doing this: the model will be used in this context to check the consistency of the preferred orientation input (*I*-ratio *vs.* Pole Figures) and not to reproduce the dilation curve or to calculate the integrity factor as a function of temperature, as done in [1,12,13]. Indeed, we will see below that hypothetical (but realistic) conditions will be fixed, and the consistency of the texture coefficients with the physical meaning of the simulation will represent the criterion for the selection of the best input number.

As stated in [1] the cordierite microcracking on cooling reduces the *a,b*-axis contributions to the bulk CTE. The amount of this contribution is called the integrity factor: for positive CTE axes *a*, *b*, it may decrease from 1 (intact state) to 0 (fully cracked state). As proposed in [1], the integrity factor (*IF*) can be estimated by the decrease of the *a,b*-axes contributions with respect to the intact state at the stress-free reference temperature (as high as 1200 °C or more). Therefore, according to the model described in [1,12], the bulk thermal expansion behavior is a function of the texture coefficients (V_a, V_b, V_c), crystallographic properties (stress-free lattice strains $\varepsilon_{a,b,c}$, elasticity

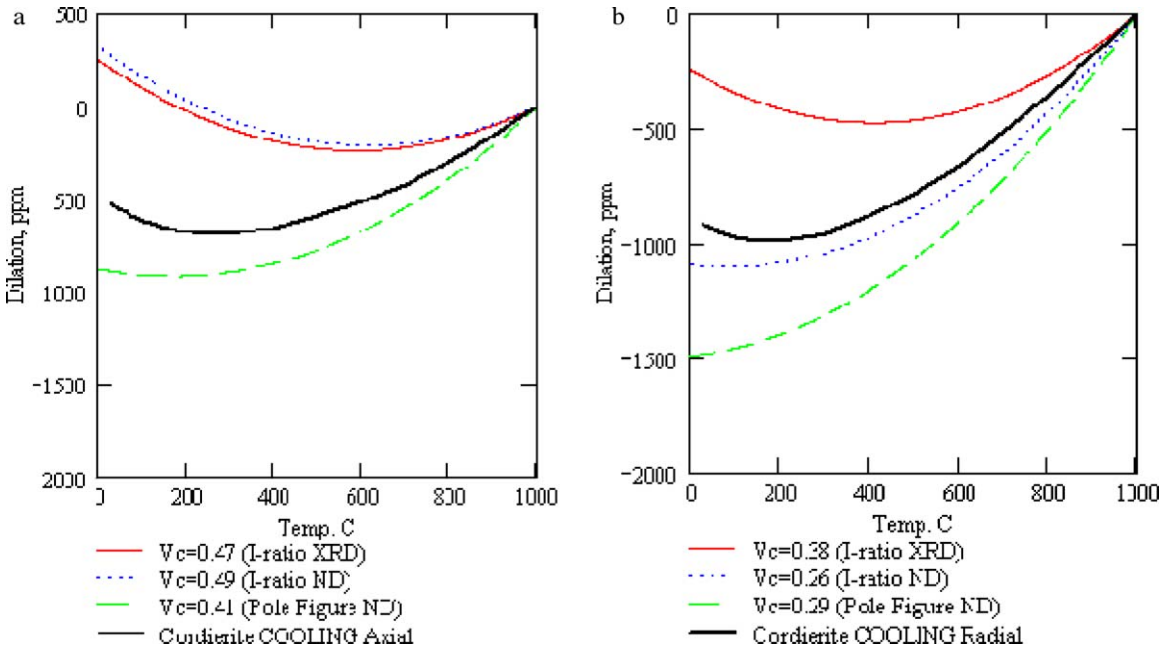

Fig. 5. Comparison between the dilation of a cellular bar as measured by dilatometry (thick solid line) in the axial (a) and radial (b) directions and the simulations of an ideal behavior at constant $IF_a = IF_b = 0.6$. The texture coefficients V_c were obtained by three methods: *I*-ratio from XRD data (thin solid curve), *I*-ratio from ND data (dotted curve) and full *c*-axis pole figure data (thick dashed curve). Lattice data from a 5 μm particle size powder were used, as reported in [12].

$E_{a,b,c}$), and integrity ($IF_{a,b,c}$):

$$\varepsilon_{bulk} = \frac{V_a \cdot \varepsilon_a \cdot E_a \cdot IF_a + V_b \cdot \varepsilon_b \cdot E_b \cdot IF_b + V_c \cdot \varepsilon_c \cdot E_c \cdot IF_c}{V_a \cdot E_a \cdot IF_a + V_b \cdot E_b \cdot IF_b + V_c \cdot E_c \cdot IF_c} \quad (22)$$

We note that the axial and radial expansions could be different due to texture as well as to different extent of microcracking. However, Fig. 6 shows that the latter was observed to be similar in both directions, since the shape of the curve of the elastic modulus (as measured by sonic resonance) vs. temperature is the same in the radial and axial direction, up to a geometrical factor, in spite of the different textures. A similar conclusion was derived in [5] from the comparison of axial and radial dilation data.

One can notice that the heating curve (bottom) at 1000 °C lies significantly below the cooling curve (top). This means that significant microcracking is left in the sample even at 1000 °C.

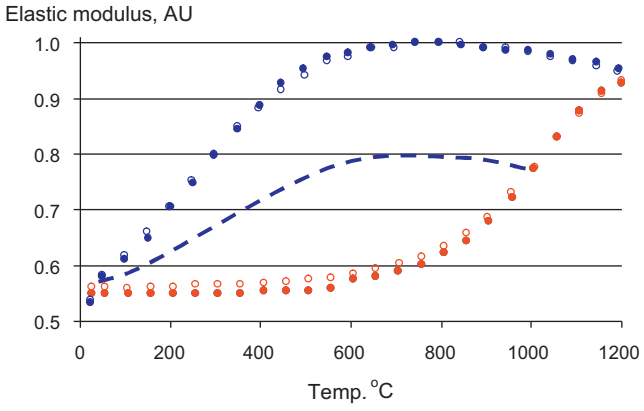

Fig. 6. Axial (solid circles) and Radial (open circles) elastic modulus normalized by max value vs. temperature, as measured by sonic resonance (see [14]) on heating (red) and cooling (blue). (For interpretation of the references to color in this figure legend, the reader is referred to the web version of the article.)

Calculations (see [1]) give an estimate of $IF_a = IF_b = 0.6$ at 1000 °C (see dashed line in Fig. 6).

These considerations imply that for cordierite

(1) On cooling from 1200° C to 800 °C texture is the only factor influencing the CTE behavior, besides the lattice dilation dependence on temperature.
(2) Microcracking shifts the dilation curve upwards, with respect to that of the intact material.

The simulated dilation curves were generated on the base of lattice expansion data of a Cordierite powder with 5 μm particle size (reported in [12]). Fig. 5 shows the comparison between the calculated dilation and the measured macroscopic dilation. One can see that small differences of the texture coefficient V_c would make a dramatic impact on the bulk CTE interpretation and prediction.

In fact, two important remarks can be made on the basis of Fig. 5:

(a) The axial and radial dilation simulations differ substantially. For the radial dilation (Fig. 5b) we cannot definitely state which of the approximations best suits the experimental data: both the neutron diffraction *I*-ratio and Pole Figure data seem to be consistent with point 2 above. On the other hand, for the axial dilation, the simulations of the ideally microcracked materials (i.e. with fixed $IF_{a,b} = 0.6$) give a CTE higher than the experimental data if the *I*-ratio data (from both Neutrons and X-rays) are used. This clearly indicates a paradox, because the contraction of an ideally microcracked body must exceed that of a real sample. Indeed, the latter obviously contains a larger and above all increasing effect of microcracking upon cooling.

(b) Only the texture coefficients evaluated from ND pole figures deliver consistent predictions in both the axial and radial directions. This consistency is confirmed by the fact that in both the Radial and the Axial directions, the difference between the simulated and the measured CTE imply a similar level of microcracking, as suggested by Fig. 6. As mentioned before, the difference between the simulated and the measured curves increases with decreasing temperature. This is because in the simulations the microcrack level (i.e. the integrity factor) is artificially kept constant.

A better numerical evaluation of the CTE is important: If we know the crystallographic texture of a sample/material, we can extract from CTE simulations some knowledge about compositional effects and internal micro-strains, and vice-versa. If a new factor appears or if one of the input data (e.g., the detailed knowledge of the sample texture) is missing, then the number of unknowns becomes too high and the predictions unsound. Although a great deal of *I*-ratio data is available at industrial level, a wide scatter of data has also been observed, certainly due to the reasons mentioned above, including the ambiguity of the definition. This implies that the *I*-ratio is *not* an exact metric of the texture. This is certainly one of the reasons why Bubeck [5] found an inconsistency between his Young's modulus data and the CTE calculations.

If texture is the physical quantity affecting the thermomechanical properties of cordierite, the *I*-ratio is, by definition, only a rough indicator of it. Even if the trends extracted by empirical treatment [5] can be correct, the number of experimental data required to do so is very large or the quantitative agreement is poor. This approach is therefore not viable if a limited amount of experimental data is available or if we want to make quantitative predictions of physical quantities (Young's modulus, CTE, etc.).

5. Conclusions

From the results and the considerations done above, we can draw the following conclusions:

(1) Neutron diffraction provides the most robust texture data, thanks to the deep penetration power of neutrons (of the order of several cm). The neutron signal averages over the whole web thickness and over several cells. It therefore yields values representative of the whole specimen. Moreover, all orientations are accounted for when averaging by means of the Popa–Bruno method.
(2) Conversely, the shallow penetration of X-rays does not allow stating sound conclusions about *bulk* properties. X-ray derived values would not be comparable with macroscopic dilation or Young's modulus data.
(3) The *I*-ratio derived from XRD is a qualitative and practical, but not a quantitative measurement of texture. It can be useful for development, quality control, but not for an input about the crystallographic orientation. For example, model predictions for common physical properties (CTE, modulus of rupture, Young's modulus, etc.) based on XRD *I*-ratio values could be very uncertain.
(4) Full *bulk* pole figure data yield sound predictions of CTE, consistent with Young's modulus.

It is finally recommended to make exclusive use of the pole figure (or ODF) information contained in neutron diffraction texture data when inputting models for physical property predictions.

Acknowledgements

Greg Merkel, Stephane Berre and Thomas Glasson of Corning Inc. Sven Vogel and Saurabh Kabra of LANSCE/LANL.

Appendix A. Derivation of the relation between *I*-ratio and V_c.

Here we simply assume that the line intensities I_i are proportional to the volume fraction of correspondingly oriented crystals (V_i)

$$I_i = A_i \cdot V_i \tag{A.1}$$

where A_i is to be a constant specific to the design of the XRD experiment only and it is independent of the sample structure or orientation. It is therefore the same for a piece of textured ceramics or for an isotropic powder, if measured on the same machine.

For a random oriented powder we would have:

$$I_i^0 = A_i \cdot V_i^0 \tag{A.2}$$

In the case of the 0 0 2 and the 1 1 0 reflections Eq. (A.2) reads:

$$I_c^0 = A_c \cdot \frac{1}{3} \quad I_{ab}^0 = A_{ab} \cdot \frac{2}{3} \tag{A.2′}$$

From which we derive:

$$A_c = 3 \cdot I_c^0 \qquad A_{ab} = \frac{3}{2} \cdot I_{ab}^0 \tag{A.3}$$

The *I*-ratio definition becomes:

$$I_{ratio} = \frac{I_{ab}}{I_{ab} + I_c} = \frac{A_{ab} \cdot V_{ab}}{A_{ab} \cdot V_{ab} + A_c \cdot V_c} = \frac{V_{ab}}{V_{ab} + 2C \cdot V_c} \tag{A.4}$$

where V_c, V_{ab} are the volume fractions of oriented domains (the quantities we want to know), and $C = {I_c}^0/{I_{ab}}^0 = {I_{002}}^0/{I_{110}}^0$. We have assumed that for an isotropic material, to which powders belong, the volume fractions of *a*,*b*, and *c* orientations are equal, so that $V_c = V_a = V_b = 1/3$ and $2\,V_c = V_{ab}$. We obtain in this case:

$$I_{powder} = \frac{I_{110}^p}{I_{110}^p + I_{002}^p} = \frac{1}{1 + C} \tag{A.5}$$

So that the constant C can be evaluated in terms of the powder *I*-ratio as

$$C = \frac{1 - I_{powder}}{I_{powder}} \tag{A.6}$$

Since $V_c + V_{ab} = 1$ in any condition, we can derive an equation for the evaluation of V_c in a solid sample from the crushed powder *I*-ratio.

$$I_{ratio} = \frac{1 - V_c}{1 - (1 - 2C)V_c} = \frac{1 - V_c}{1 - (2I_{powder} - 1/I_{powder}) \cdot V_c} \tag{A.7}$$

Eq. (A.5) has the solution

$$V_c = \frac{1 - I_{ratio}}{1 - (2I_{powder} - 1/I_{powder}) \cdot I_{ratio}} \tag{A.8}$$

This demonstrates the statement Eq. (2).

The calibrated values of the *I*-ratio can be calculated in the following manner:

If $I_{theory} = 2/3$ (Lachman's definition, Eq. (1′)), by substituting in eq. (A.7) we get:

$$I^0_{ratio} = \frac{1 - V_c}{1 - (V_c/2)} \tag{A.9}$$

and therefore

$$V_c = \frac{2 \cdot (1 - I^0_{ratio})}{2 - I^0_{ratio}} \tag{A.9′}$$

Upon substitution of this V_c value in Eq. (A.7) and some algebra, we get:

$$I_{ratio} = \frac{I^0_{ratio}}{(3 - (2/I_{powder})) \cdot I^0_{ratio} + 2 \cdot ((1/I_{powder}) - 1)} \tag{A.10}$$

This equation can be inverted to give the calibrated *I*-ratio ($I_{ratio}{}^0$) as a function of the measured *I*-ratio (I_{ratio}) as

$$I^0_{ratio} = \frac{2 \cdot ((1/I_{powder}) - 1) \cdot I_{ratio}}{1 - (3 - (2/I_{powder})) \cdot I_{ratio}} \tag{A.10′}$$

Eqs. (A.10) and (A.10′) satisfy the boundary condition: $I_{ratio}{}^0 = I_{ratio}$, if the measured reference has effectively $I_{powder} = 2/3$.

Analogously, if $I_{theory} = 3/4$ (Bubeck's use, Eq. (1″)), by substituting in Eq. (A.7) we get:

$$I^0_{ratio} = \frac{1 - V_c}{1 - (2V_c/3)} \tag{A.11}$$

and therefore

$$V_c = \frac{3 \cdot (1 - I^0_{ratio})}{3 - 2 \cdot I^0_{ratio}} \tag{A.11′}$$

Upon substitution of this V_c value in Eq. (A.7) and some algebra, we get:

$$I_{ratio} = \frac{I^0_{ratio}}{(4 - (3/I_{powder})) \cdot I^0_{ratio} + 3 \cdot ((1/I_{powder}) - 1)} \tag{A.12}$$

This equation can be inverted to give the calibrated *I*-ratio ($I_{ratio}{}^0$) as a function of the measured *I*-ratio (I_{ratio}) as

$$I^0_{ratio} = \frac{3 \cdot ((1/I_{powder}) - 1) \cdot I_{ratio}}{1 - (4 - (3/I_{powder})) \cdot I_{ratio}} \tag{A.12′}$$

Also in this case, Eqs. (A.12) and (A.12′) satisfy the boundary condition: $I_{ratio}{}^0 = I_{ratio}$, if the measured reference has effectively $I_{powder} = 3/4$.

Appendix B. Derivation of the relation between pole figures and V_c

Here we will derive the texture coefficients for orthotropic crystals with anisotropic properties along the crystal axes: $a \neq b \neq c$.

The laboratory coordinate system *XYZ* and the grain coordinate system *xyz* are explicitly related by the Euler angles ψ, θ, ϕ. For instance, the transformation of strain from one system to another is given by transformation matrix $T(\psi, \theta, \varphi)$ made by 3 rotations T_1, T_2, T_3 as given below [15]

$$T_1(\psi) = \begin{pmatrix} \cos(\psi) & \sin(\psi) & 0 \\ -\sin(\psi) & \cos(\psi) & 0 \\ 0 & 0 & 1 \end{pmatrix}$$

$$T_2(\theta) = \begin{pmatrix} \cos(\theta) & 0 & \sin(\theta) \\ 0 & 1 & 0 \\ -\sin(\theta) & 0 & \cos(\theta) \end{pmatrix}$$

$$T_3(\varphi) = \begin{pmatrix} 1 & 0 & 0 \\ 0 & \cos(\varphi) & \sin(\varphi) \\ 0 & -\sin(\varphi) & \cos(\varphi) \end{pmatrix} \tag{B.1}$$

So that the total transformation matrix can be written as $T(\psi, \theta, \phi) = T_1(\psi) \cdot T_2(\theta) \cdot T_3(\phi)$ such that:

$$T(\psi, \theta, \phi) \rightarrow \begin{pmatrix} \cos(\psi) \cdot \cos(\phi) - \sin(\psi) \cdot \cos(\theta) \cdot \sin(\phi) & \cos(\psi) \cdot \sin(\phi) + \sin(\psi) \cdot \cos(\theta) \cdot \cos(\phi) & \sin(\psi) \cdot \sin(\theta) \\ -\sin(\psi) \cdot \cos(\phi) - \cos(\psi) \cdot \cos(\theta) \cdot \sin(\phi) & -\sin(\psi) \cdot \sin(\phi) + \cos(\psi) \cdot \cos(\theta) \cdot \cos(\phi) & \cos(\psi) \cdot \sin(\theta) \\ \sin(\theta) \cdot \sin(\phi) & -\sin(\theta \cdot \cos(\phi)) & \cos(\theta) \end{pmatrix} \tag{B.2}$$

By using Eq. (7), we can easily prove that Eq. (9) holds by the fact that

$$\varepsilon(\psi,\theta,\phi,0,01)\cdot\varepsilon_c-\varepsilon(\psi,\theta,\phi,0,0,\varepsilon_c)\rightarrow\begin{pmatrix}0&0&0\\0&0&0\\0&0&0\end{pmatrix} \tag{B.3}$$

For a single grain, the contributions of the c-axis orientation, rotated by ψ, θ, ϕ in the laboratory system, is given by texture coefficient v_c, which is equal to:

$$T(\psi,\theta,\phi)\cdot\varepsilon_g(0,0,1)\cdot T(\psi,\theta,\phi)^T\rightarrow\begin{pmatrix}\sin^2(\psi)\cdot\sin^2(\theta) & \sin(\psi)\cdot\sin^2(\theta)\cdot\cos(\psi) & \sin(\psi)\cdot\sin(\theta)\cdot\cos(\theta)\\ \sin(\psi)\cdot\sin^2(\theta)\cdot\cos(\psi) & \cos^2(\psi)\cdot\sin^2(\theta) & \cos(\psi)\cdot\sin(\theta)\cdot\cos(\theta)\\ \sin(\psi)\cdot\sin(\theta)\cdot\cos(\theta) & \cos(\psi)\cdot\sin(q)\cdot\cos(\theta) & \cos^2(\theta)\end{pmatrix} \tag{B.4}$$

If we now take the polycrystalline average Eq. (11), we can write

$$\begin{aligned}\varepsilon_{\text{macro}} &= \frac{1}{8\pi^2}\cdot\int_0^{2\pi}\int_0^{\pi}\int_0^{2\pi} v_a(\psi,\theta,\phi)\cdot f(\psi,\theta,\phi)\cdot\\ &\quad\times\sin(\theta)\,\mathrm{d}\psi\,\mathrm{d}\theta\,\mathrm{d}\phi\cdot\varepsilon_a+\frac{1}{8\pi^2}\cdot\\ &\quad\times\int_0^{2\pi}\int_0^{\pi}\int_0^{2\pi} v_b(\psi,\theta,\phi)\cdot f(\psi,\theta,\phi)\cdot\\ &\quad\times\sin(\theta)\,\mathrm{d}\psi\,\mathrm{d}\theta\,\mathrm{d}\phi\cdot\varepsilon_b+\frac{1}{8\pi^2}\cdot\\ &\quad\times\int_0^{2\pi}\int_0^{\pi}\int_0^{2\pi} v_c(\psi,\theta,\phi)\cdot f(\psi,\theta,\phi)\cdot\\ &\quad\times\sin(\theta)\,\mathrm{d}\psi\,\mathrm{d}\theta\,\mathrm{d}\phi\cdot\varepsilon_c\\ &= \frac{1}{8\pi^2}\cdot\int_0^{2\pi}\int_0^{\pi}\int_0^{2\pi}\begin{pmatrix}1&0&0\\0&1&0\\0&0&1\end{pmatrix}\cdot f(\psi,\theta,\phi)\cdot\cdot\\ &\quad\times\sin(\theta)\,\mathrm{d}\psi\,\mathrm{d}\theta\,\mathrm{d}\phi = V_a\cdot\varepsilon_a+V_b\cdot\varepsilon_b+V_c\cdot\varepsilon_c\end{aligned} \tag{B.5}$$

and demonstrate that the polycrystalline texture coefficients V_a, V_b, V_c satisfy the rule $V_a+V_b+V_c=1$ by using Eq. (13):

$$\begin{aligned}V_a+V_b+V_c &= \frac{1}{8\pi^2}\iiint f(\psi,\theta,\phi)\cdot\begin{pmatrix}1&0&0\\0&1&0\\0&0&1\end{pmatrix}\cdot d\psi\cdot d\theta\cdot d\phi\\ &= \frac{1}{8\pi^2}\begin{pmatrix}1&0&0\\0&1&0\\0&0&1\end{pmatrix}\cdot\iiint f(\psi,\theta,\phi)\cdot d\psi\cdot d\theta\cdot d\phi\\ &= \frac{1}{8\pi^2}\begin{pmatrix}1&0&0\\0&1&0\\0&0&1\end{pmatrix}\end{aligned} \tag{B.6}$$

This result proves that for any texture function $f(\psi,\theta,\phi)$ and any direction (ax, rad, hoop) the coefficients will follow Eq. (B.6)

For example in the isotropic case $f(\psi,\theta,\phi)=\text{const}$, a straightforward calculation yields

$$V_a:=\frac{1}{8\pi^2}\int_0^2\int_0^{\pi}\int_0^{2\pi} v_a(\psi,\theta,\phi)_{1,1}\cdot f\cdot\sin(\theta)d\psi\,d\theta\,d\phi$$

$$V_a=0.333\quad V_b=0.333\quad V_c=0.333 \tag{B.7}$$

References

1. Efremov AM. Impact of domain anisotropy on isotropic microcrystalline material. *Phil Mag* 2006;**86**:5431–40.
2. Turner PS. Thermal-expansion stresses in reinforced plastics. *J Res Natl Bureau Stand* 1946;**37**:239–50.
3. Bruno G, Vogel S. Calculation of the average coefficient of thermal expansion in oriented cordierite polycrystals. *J Am Ceram Soc* 2008;**91**: 2646–52.
4. Lachman IM, Bagley RD, Lewis RM. Thermal expansion of extruded cordierite ceramics. *Bull Amer Ceram Soc* 1981;**60**:202–5.
5. Bubeck C. Direction dependent mechanical properties of extruded cordierite honeycombs. *J Eur Ceram Soc* 2009;**29**:3113–9.
6. ICSD (Inorganic Crystal Structure database), NIST, Washington DC, USA and Fachinformationszentrum Karlsruhe (FIZ), Germany. JCPDS, International Centre for Diffraction Data; 2009.
7. Popa NC, Balzar D. Elastic strain and stress determination by Rietveld refinement: generalized treatment for textured polycrystals for all Laue classes. *J Appl Cryst* 2001;**34**:187–95.
8. Wenk HR, Lutterotti L, Vogel S. Texture analysis with the new HIPPO TOF diffractometer. *Nucl Inst Meth A* 2003;**515**:575–88.
9. Maslen EN, X-ray absorption in International tables of X-ray Crystallography, vol. C; 2006.
10. Physical Values, Atom Izdat; 1991 (Russian).
11. Bunge HJ. *Texture analysis in materials science*. London: Butterworth; 1982.
12. Bruno G, Efremov AM, Clausen B, Simkin V, Balagurov AM, Brown DW, et al. On the stress free lattice expansion of cordierite. *Acta Mater* 2010;**58**:1994–2003.
13. Bruno G, Efremov AM, Brown DW. Evidence for and calculation of the micro-strain in porous synthetic cordierite. *Scr Mater* 2010;**63**: 285–8.
14. ASTM standard C1198-01. Dynamic Young's modulus, Shear modulus, and Poisson's ratio for advanced ceramics by sonic resonance; 1998.
15. Talpaert Y. *Tensor analysis and continuum mechanics*. Dordrecht: Kluwer Academics; 2002.